Daurinol, a catalytic inhibitor of topoisomerase IIα, suppresses SNU-840 ovarian cancer cell proliferation through cell cycle arrest in S phase

KYUNGSU KANG[1*], CHU WON NHO[1*], NAM DOO KIM[2], DAE-GEUN SONG[1], YOUNG GYUN PARK[1], MINKYUN KIM[4], CHEOL-HO PAN[1], DONGYUN SHIN[3], SEUNG HYUN OH[3] and HO-SUK OH[5]

[1]Functional Food Center, Korea Institute of Science and Technology, Gangneung; [2]New Drug Development Center, Daegu-Gyeongbuk Medical Innovation Foundation, Daegu; [3]College of Pharmacy, Gachon University, Incheon; [4]Department of Agricultural Biotechnology, Seoul National University, Seoul; [5]Department of Internal Medicine, Gangneung Asan Hospital, University of Ulsan College of Medicine, Gangneung, Republic of Korea

Received January 28, 2014; Accepted March 29, 2014

DOI: 10.3892/ijo.2014.2442

Abstract. Daurinol, a lignan from the ethnopharmacological plant *Haplophyllum dauricum*, was recently reported to be a novel topoisomerase II inhibitor and an alternative to the clinical anticancer agent etoposide based on a colorectal cancer model. In the present study, we elucidated the detailed biochemical mechanism underlying the inhibition of human topoisomerase IIα by daurinol based on a molecular docking study and *in vitro* biochemical experiments. The computational simulation predicted that daurinol binds to the ATP-binding pocket of topoisomerase IIα. In a biochemical assay, daurinol (10-100 μM) inhibited the catalytic activity of topoisomerase IIα in an ATP concentration-dependent manner and suppressed the ATP hydrolysis activity of the enzyme. However, daurinol did not inhibit topoisomerase I activity, most likely because topoisomerase I does not contain an ATP-binding domain. We also evaluated the anti-proliferative activity of daurinol in ovarian, small cell lung and testicular cancer cells, common target cancers treated with etoposide. Daurinol potently inhibited SNU-840 human ovarian cancer cell proliferation through cell cycle arrest in S phase, while etoposide induced G2/M phase arrest. Daurinol induced the increased expression of cyclin E, cyclin A and E2F-1, which are important proteins regulating S phase initiation and progression. Daurinol did not induce abnormal cell and nuclear enlargement in SNU-840 cells, in contrast to etoposide. Based on these data, we suggest that daurinol is a potential anticancer drug candidate for the treatment of human ovarian cancer with few side effects.

Correspondence to: Professor Ho-Suk Oh, Department of Internal Medicine, Gangneung Asan Hospital, University of Ulsan College of Medicine, 415 Bangdong-ri, Gangneung-si, Gangwon-do 210-711, Republic of Korea
E-mail: hosukoh@hanmail.net

*Contributed equally

Key words: daurinol, topoisomerase IIα inhibitor, ovarian cancer, ATP binding pocket, secondary leukemia

Introduction

Topoisomerases are essential enzymes in all organisms that are involved in the topological homeostasis of DNA molecules during DNA replication, transcription and chromosomal segregation. Topoisomerases are classified into two classes, topoisomerase I and II, which create single and double-strand breaks, respectively. Because topoisomerases are crucial enzymes in DNA replication, they have served as primary targets for the development of anticancer agents (1,2). Topoisomerase II inhibitors such as etoposide, teniposide and doxorubicin have been extensively used in clinical cancer treatment. However, these agents also have undesirable side effects, including immunosuppression, myelosuppression, gastrointestinal toxicity and the development of secondary leukemia (3). Thus, the discovery of new topoisomerase inhibitors with fewer side effects from natural products has received a great deal of attention (4,5).

Daurinol is a natural arylnaphthalene lignan isolated from the traditional medicinal plant *Haplophyllum dauricum* (6). According to an ethnopharmacological study, this plant has been used to treat tumors in Russia (7). The chemical structure of daurinol is similar to that of the clinical anticancer agent VP-16 (also known as etoposide phosphate). Recently, we suggested that daurinol could be a promising antitumor agent with minimal side effects, compared to etoposide, based on *in vitro* and *in vivo* results. Daurinol suppressed the growth of human colorectal cancer cells through the inhibition of human topoisomerase IIα *in vitro* and dramatically inhibited the growth of HCT116 tumors in a nude mouse xenograft model. Moreover, daurinol did not show severe side effects such as loss of body weight and hematological toxicity, i.e., loss of white blood cells and red blood cells, and decreased hemoglobin content (5).

However, this previous study revealed some limitations of daurinol that must be resolved to develop this agent as a novel alternative to etoposide in clinical trials. First, the availability of natural daurinol from the plant *H. dauricum* is limited because its content is quite low (0.013% of the plant dry weight) (6). Second, daurinol inhibits human topoisomerase IIα activity in the millimolar range (5). We neither elucidated the inhibitory activity against other topoisomerases, including topoisomerase I, nor identified the detailed biochemical mechanism underlying the daurinol-induced inhibition of topoisomerase IIα. Last but most important, we did not examine its effect on other cancer cell types besides colorectal cancer, even though etoposide is also frequently used to treat other cancers such as ovarian, small-cell lung and testicular cancer (3,8).

To address these limitations, in the present study, we used synthetic daurinol prepared by a regioselective chemical synthesis. In addition, we have proposed a biochemical mechanism underlying the inhibitory action of daurinol against human topoisomerase IIα based on a computational molecular docking study and biochemical experiments. Finally, we tested the anticancer activity of synthetic daurinol against human ovarian, small-cell lung and testicular cancer cells and investigated the effects of daurinol on cell cycle distribution and cell morphology in the selected cancer cells in comparison to etoposide.

Materials and methods

Reagents. Daurinol used in this study was chemically synthesized according to recently reported methods (9). Natural daurinol was isolated from *Haplophyllum dauricum* as previously described (6). Dimethyl sulfoxide (DMSO), etoposide, novobiocin, propidium iodide (PI) and ATP disodium salt were purchased from Sigma (St. Louis, MO, USA). Camptothecin was purchased from TopoGEN, Inc. (Port Orange, FL, USA). Daurinol, etoposide and camptothecin were dissolved in DMSO for cellular treatment. Antibodies against E2F-1 (3742), cyclin A (4656) and Cdk4 (2906) were purchased from Cell Signaling Technology (Danvers, MA, USA). Antibodies against Cdk2 (sc-163), cyclin E (sc-247), cyclin D1 (sc-753) and β-actin (sc-47778) were purchased from Santa Cruz Biotechnology (Santa Cruz, CA, USA). Secondary anti-rabbit and anti-mouse antibodies were purchased from Santa Cruz Biotechnology.

Molecular docking analysis. The crystal structure of human topoisomerase IIα (ATP2ATPase) complexed with AMPPNP (a non-hydrolyzable ATP analog) from the Protein Data Bank (PDB code 1ZXM) was used for the docking simulation. Daurinol was built using the Maestro build panel and minimized using the impact module of Maestro in the Schrödinger suite program. The starting coordinates of the ATP2ATPASE were further modified for the prediction of daurinol binding. The protein structure was minimized using the Protein Preparation Wizard by applying an OPLS force field. For grid generation, the binding site was defined as the centroid of the AMPPNP. Ligand docking into the active site of ATP2ATPASE was performed using the Schrödinger docking program Glide (Schrödinger, Inc., USA). Energy-minimized daurinol was docked into the prepared receptor grid. The best-docked poses were selected based on the lowest Glide scores. The molecular graphics of the inhibitor-binding pocket and refined docking model for daurinol were generated using the PyMol package (http://www.pymol.org).

Measurement of human topoisomerase IIα catalytic activity. The inhibitory activity of daurinol against human topoisomerase IIα was measured using the Topoisomerase II Drug Screening kit (TopoGEN, Inc.). The standard reaction mixture (20 μl) contained 250 ng of supercoiled DNA (pHOT1), 0.7 μl of topoisomerase IIα, and different concentrations of ATP (0.5, 1 or 2 mM) and the tested compounds dissolved in DMSO. The final concentration of DMSO was 1%, and the topoisomerase II poison etoposide was used as a positive control. Reactions were initiated by the addition of the supercoiled DNA substrate. The reaction mixture was incubated at 37˚C for 30 min. Other procedures were performed as described previously (5).

Measurement of human topoisomerase I catalytic activity. The inhibitory activity of daurinol against human topoisomerase I was measured using the Topoisomerase I Assay kit (TopoGEN, Inc.). The standard reaction mixture (20 μl) contained 10 mM Tris-HCl (pH 7.9), 1 mM EDTA, 150 mM NaCl, 0.1% bovine serum albumin (BSA), 0.1 mM spermidine, 5% glycerol, 250 ng of supercoiled DNA (pHOT1), 0.7 μl of topoisomerase I, and the test compound dissolved in DMSO. The final concentration of DMSO was 1%, and the topoisomerase I poison camptothecin was used as a positive control. Reactions were initiated by the addition of the supercoiled DNA substrate. The reaction mixture was incubated at 37˚C for 30 min, and 2 μl of 10% sodium dodecyl sulfate was added to stop the reaction. Additional procedures were performed using procedures similar to the topoisomerase II assay, as described previously (5).

ATPase activity assay. The DNA-dependent ATP hydrolysis activity of human topoisomerase IIα was determined by quantifying hydrolyzed inorganic phosphate using the malachite green assay with slight modifications (10-12). Briefly, the standard reaction mixture (20 μl) contained 50 mM Tris-HCl (pH 8.0), 150 mM NaCl, 10 mM $MgCl_2$, 0.5 mM dithiothreitol, 30 μg/ml BSA, 200 ng of supercoiled DNA (pHOT-1), 2.0 μl of human topoisomerase IIα (TopoGEN, Inc.); and 100 μM daurinol or 400 μM novobiocin dissolved in DMSO. The final concentration of DMSO was 1%, and novobiocin was used as a positive control (12,13). The reaction was initiated by adding ATP at a final concentration of 2 mM (Sigma) and was incubated at 37˚C for 30 min. The reaction was stopped by the addition of the Lanzetta reagent (80 μl, freshly prepared mixture of 0.035% malachite green-HCl and 4.2% ammonium molybdate in 4 N HCl at a ratio of 3:1 and 0.2% CHAPS), and the color development was read immediately using a Synergy HT Multi-Mode Microplate Reader (BioTek Instruments, Winooski, VT, USA) at 620 nm. The amount of inorganic phosphate was calculated using a phosphate (potassium dihydrogen phosphate, KH_2PO_3) standard curve. Enzyme activity was expressed as μM phosphate produced per min reaction.

Cell culture. SK-OV-3 and NIH:OVCAR-3 human ovarian cancer; and NTERA-2 cl.D1 (NT2-D1), NCCIT human testicular cancer cell lines were obtained from American Type Culture Collection (ATCC; Rockville, MD, USA). The SNU-840 human ovarian cancer; and NCI-H69, NCI-H146, NCI-H187 and NCI-H417 human small-cell lung cancer cell lines were obtained from the Korean Cell Line Bank (Seoul, Korea). These cells were cultured in RPMI-1640 supplemented with 25 mM HEPES, 10% (v/v) heat-inactivated fetal bovine serum (FBS), 100 U/ml penicillin and 100 μg/ml streptomycin. Cells were maintained at sub-confluence in a 95% air and 5% CO_2 humidified atmosphere at 37˚C.

Measurement of anti-proliferative activity. Cancer cells ($5x10^3$ cells/well) were plated in 96-well plates, incubated at 37˚C for 24 h, and treated with daurinol for 48 h. Cell viability was determined using the EZ-Cytox cell viability assay kit (Daeil Lab Service, Ltd., Seoul), as previously described (14).

Cell cycle analysis. NIH:OVCAR-3 ($5x10^5$ cells/well), SNU-840 ($3x10^5$ cells/well) and NCCIT ($3x10^5$ cells/well) cells were plated in 6-well plates, incubated at 37˚C for 24 h, and treated with daurinol or etoposide for 24 and 48 h. The cells were stained with PI, and their DNA contents were analyzed using a FACSCalibur flow cytometer (Becton-Dickinson, San Jose, CA, USA) and Modfit LT V3.0 software (Verity Software House, Topsham, ME, USA) as previously described (5).

Western blot analysis. SNU-840 cells ($5x10^5$) were seeded on 60-mm dishes, incubated for 24 h, and then treated with daurinol for 24 and 48 h. Additional procedures were performed as previously described (15). The relative protein expression was measured by densitometry.

Evaluation of cell and nuclear size. To evaluate the effect of daurinol and etoposide on cell and nuclear size, we performed fluorescence pulse signal analysis of PI-stained SNU-840 cells as previously described (15,16). The treatment and flow cytometric DNA content analysis were performed as described above in the section of cell cycle analysis. FSC-H and FL2-W values, which correlate with cell and nuclear size, respectively, were measured using flow cytometry. The mean values of FSC-H and FL2-W were calculated using the histogram statistics tool from CellQuest Pro software (Becton-Dickinson). To compare the FSC-H and FL2-W distributions of the control and chemical-treated cells, we used the Kolmogorov-Smirnov statistics tools from CellQuest Pro software. We also observed SNU-840 cell morphology after treatment with daurinol or etoposide using an Olympus CK40 phase contrast microscope (Tokyo, Japan).

Statistical analysis. The values represent the mean ± standard deviation (SD). Statistical analyses were performed using GraphPad Prism 5 software (La Jolla, CA, USA). A paired two-tailed Student's t-test was used to compare the IC_{50} values of daurinol and etoposide in each cell line. One-way analysis of variance (ANOVA) followed by Dunnett's or Tukey's multiple comparison test was used to analyze all other data. $P<0.05$ was considered statistically significant.

Results

Synthetic daurinol and natural daurinol have equivalent anticancer activity in HCT116 cells. Because only a minute amount of natural daurinol is present in the plant *H. dauricum*, large-scale production of daurinol is one of the key hurdles to its development as a clinical anticancer drug. Thus, we prepared synthetic daurinol using recently described regio-selective chemical synthesis methods (9) and tested its anticancer activity in various cancer cells, including HCT116 cells. The anti-proliferative activity (IC_{50} value) of synthetic daurinol was equivalent to that of natural daurinol in HCT116 cells. In addition, synthetic daurinol also clearly induced cell cycle arrest at S phase in HCT116 cells (data not shown). These results were in accordance with our previous report (5). Based on these data, we used synthetic daurinol as a substitute for natural daurinol in the present study.

Molecular docking predicts that daurinol binds to the ATP-binding site of human topoisomerase IIα. We used molecular docking simulations to evaluate the biochemical mechanism underlying the inhibitory activity of daurinol against human topoisomerase IIα. The results indicated the formation of hydrogen-bond interactions between daurinol and the polar side chains in the catalytic site of topoisomerase IIα. As shown in Fig. 1A, the model of daurinol bound to topoisomerase IIα indicated the following important interactions: the hydrogen bond between the benzodioxol functional group of daurinol and the Lys168 side chain of the enzyme and the interactions between the naphthofuranone ring of daurinol and water in topoisomerase IIα (Fig. 1A and C). Most importantly, the binding site of daurinol is identical to the binding site of AMP-PNP, a non-hydrolyzable ATP analog (Fig. 1B). Therefore, we speculated that daurinol inhibits human topoisomerase IIα by targeting its ATPase domain.

Daurinol inhibits human topoisomerase IIα catalytic activity in an ATP concentration-dependent manner. To verify the hypothesis from the molecular docking study, we measured human topoisomerase IIα activity in the presence of different concentrations of ATP. We previously reported the inhibitory activity of daurinol against topoisomerase IIα to be in the millimolar range (5). To more accurately evaluate topoisomerase IIα inhibition, we tested micromolar concentrations of daurinol in this study. As shown in Fig. 2, micromolar concentrations of daurinol potently inhibited the catalytic activity of human topoisomerase IIα and prevented the relaxation of the supercoiled DNA substrate. Notably, increasing the ATP concentration resulted in decreased inhibitory activity. When the enzyme reaction was performed in the presence of 0.5 mM ATP, daurinol inhibited the enzyme activity at concentrations of 10-100 μM. However, in the presence of 2 mM ATP, only 100 μM daurinol clearly inhibited the catalytic activity of topoisomerase IIα (Fig. 2). These data are in agreement with the molecular docking predictions.

Daurinol does not inhibit human topoisomerase I catalytic activity. To further confirm that daurinol inhibits human topoisomerase IIα by targeting the ATP-binding pocket, we measured the inhibitory activity of daurinol against human

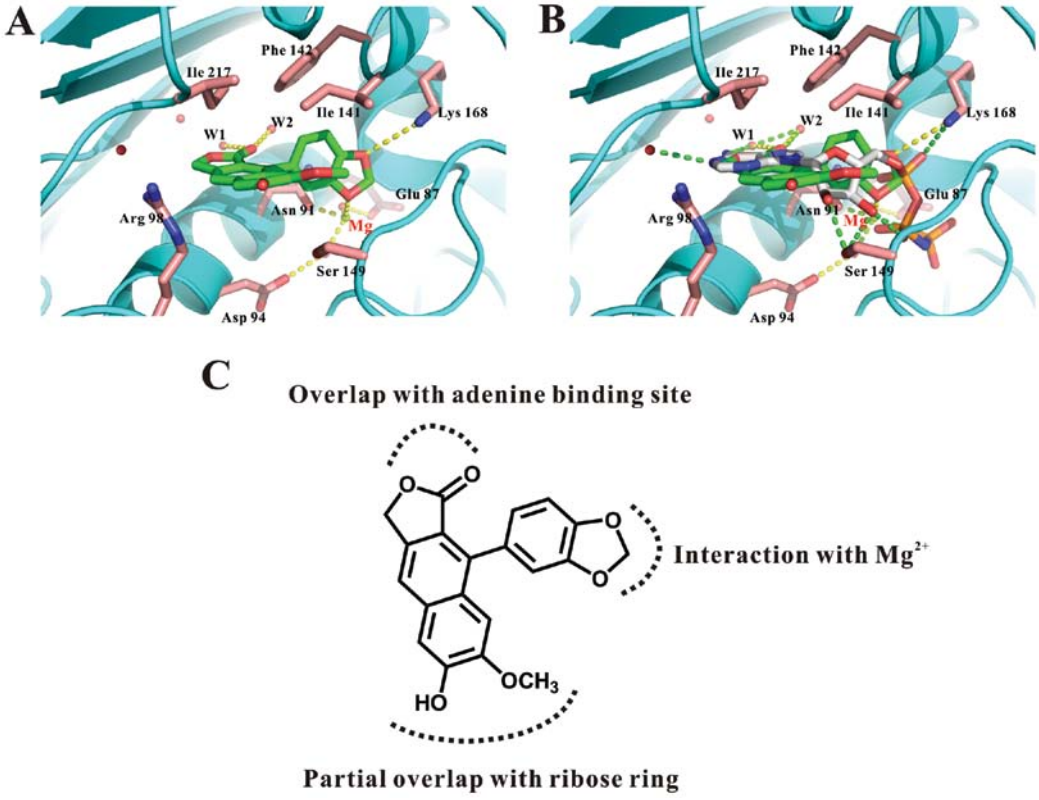

Figure 1. Predicted interaction between daurinol and human topoisomerase IIα based on the computational simulation. (A) Molecular docking of daurinol to the ATP-binding domain of topoisomerase IIα. (B) Superimposition of daurinol and AMP-PNP (a non-hydrolyzable ATP analog) in the ATP-binding domain of topoisomerase IIα. The dashed lines represent hydrogen bonds. (C) The functional groups of daurinol interact or overlap with the other ligand, AMP-PNP in the molecular docking model.

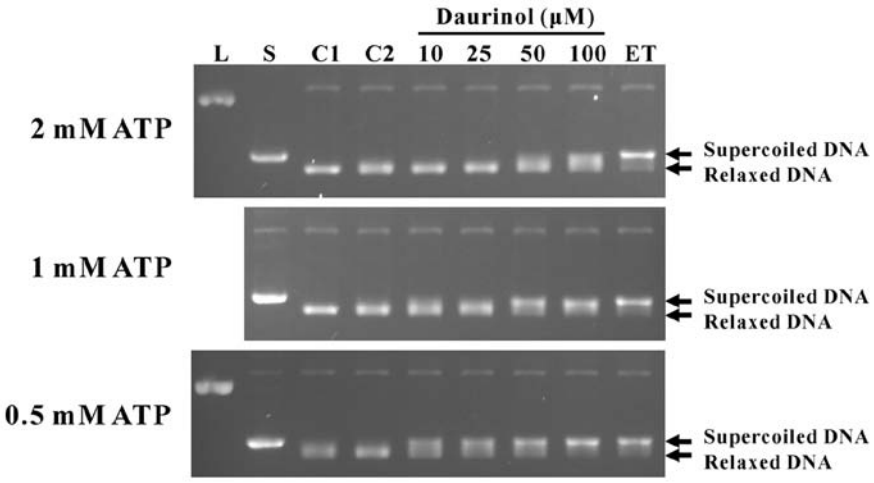

Figure 2. Effect of ATP concentration on the inhibition of human topoisomerase IIα by daurinol. The supercoiled DNA substrate (pHOT1) was incubated with topoisomerase IIα, daurinol (10-100 μM) or etoposide (ET, 200 μM) in the presence of different concentrations of ATP (0.5, 1 or 2 mM). DNA relaxation was evaluated by 1% agarose gel electrophoresis in the presence of ethidium bromide. L, linear pHOT1 DNA marker; S, supercoiled pHOT1; C1, supercoiled pHOT1 + topoisomerase IIα; C2, supercoiled pHOT1 + topoisomerase IIα + 1% DMSO.

topoisomerase I using an *in vitro* biochemical assay. Because topoisomerase I does not contain an ATPase domain and its catalytic activity is ATP-independent (17), we anticipated that daurinol, which targets ATP binding, would not inhibit human topoisomerase I activity. As expected, daurinol did not severely inhibit the catalytic activity of topoisomerase I at the concentrations (up to 100 μM) tested, whereas camptothecin (a topoisomerase I inhibitor) clearly inhibited the catalytic activity of topoisomerase I (Fig. 3).

Daurinol inhibits the ATP hydrolysis activity of human topoisomerase IIα. We also measured the ATP hydrolysis activity

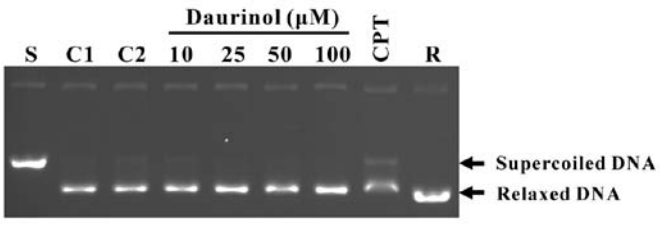

Figure 3. Effect of daurinol on human topoisomerase I activity. The supercoiled DNA substrate (pHOT1) was incubated with topoisomerase I; and daurinol (10-100 μM) or camptothecin (100 μM). DNA relaxation was evaluated by 1% agarose gel electrophoresis in the presence of ethidium bromide. S, supercoiled pHOT1; C1, supercoiled pHOT1 + topoisomerase I; C2, supercoiled pHOT1 + topoisomerase I + 1% DMSO; R, relaxed pHOT1 DNA marker.

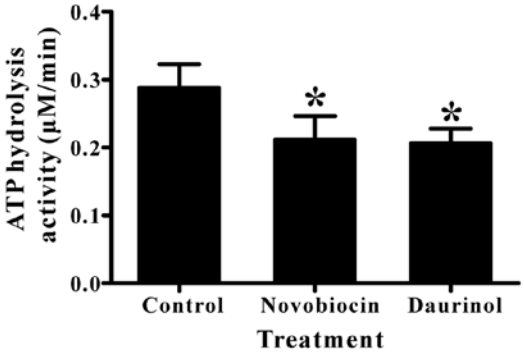

Figure 4. Effect of daurinol on the ATP hydrolysis activity of human topoisomerase IIα. Supercoiled DNA (pHOT1), 2 mM ATP and topoisomerase IIα were incubated for 30 min. The amount of inorganic phosphate produced was determined using the malachite green assay as described in Materials and methods. Statistics are based on ANOVA followed by Dunnett's test; *P<0.05 compared with control.

of human topoisomerase IIα in the presence or absence of daurinol using the malachite green method to confirm that daurinol inhibits topoisomerase IIα by targeting its ATPase domain. Both daurinol and novobiocin (a topoisomerase II inhibitor that blocks ATP binding) (12,18) significantly inhibited the ATP hydrolysis activity of human topoisomerase IIα (Fig. 4). Taken together, these results demonstrate that micromolar daurinol selectively inhibits human topoisomerase IIα by targeting the ATPase domain.

Daurinol inhibits SNU-840 human ovarian cancer cells in vitro. Next, we measured the anti-proliferative activity of daurinol in various human cancer lines. We previously reported the anticancer activity of daurinol in colorectal cancer cells compared to etoposide. However, etoposide is usually used to treat various cancers such as ovarian, small cell lung, and testicular cancer rather than colorectal cancer. Therefore, to evaluate the overwhelming anticancer effects of daurinol as a novel alternative to etoposide, we measured the anti-proliferative activity in other cancer cell types. We tested a total of 9 different cell lines (3 ovarian cancers, 4 small cell lung cancers and 2 testicular cancers). Daurinol potently inhibited ovarian cancer cell lines, particularly NIH:OVCAR-3 and SNU-840 cells, compared to etoposide. Daurinol also inhibited small-cell lung cancer cells, but the potency of daurinol was similar to or weaker than that of etoposide (Table I). Because the strongest anti-proliferative activity of daurinol was observed in SNU-840 cells compared to etoposide, we selected SNU-840 for further investigation.

Daurinol induces cell cycle arrest in S phase in SNU-840 cells. We evaluated the effects of daurinol on cell cycle distribution in human ovarian cancer cells using flow cytometric DNA content analysis. Treatment with daurinol for 24 or 48 h apparenly induced cell cycle arrest in S phase. By contrast, etoposide significantly induced cell cycle arrest in the G2/M phase (Fig. 5). Daurinol also induced an accumulation of the cell population in S phase in NCCIT human testicular cancer cells (data not shown).

Table I. Antiproliferative activity of daurinol and etoposide in human ovary, small-cell lung and testicular cancer cell lines.

		IC_{50} (μM)		
Cancer type	Cell line	Daurinol	Etoposide	Statistical difference
Ovarian	SK-OV-3	15.3±2.7	10.2±0.9	*
	NIH:OVCAR-3	4.6±0.4	47.7±3.2	**
	SNU-840	0.6±0.2	37.5±3.3	**
Small cell lung cancer	NCI-H69	3.3±1.0	8.8±2.4	
	NCI-H146	4.0±1.3	2.7±1.4	
	NCI-H187	4.6±0.1	0.3±0.0	***
	NCI-H417	7.2±1.1	7.8±1.9	
Testicular	NT2-D1	3.3±0.3	0.1±0.0	**
	NCCIT	0.7±0.3	18.1±3.0	**

IC_{50}, concentration that inhibits cell proliferation by 50%. Cells were treated with daurinol or etoposide for 48 h. The data are expressed as the mean ± SD of three independent experiments. Statistics were based on Student's t-test of the difference between daurinol and etoposide; *P<0.05, **P<0.01 and ***P<0.001.

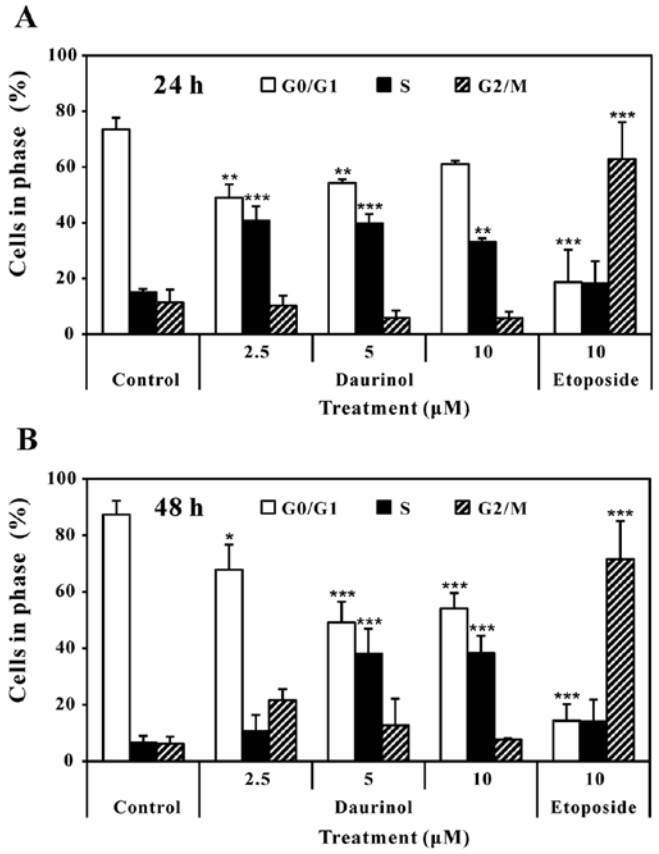

Figure 5. Effect of daurinol and etoposide on the cell cycle distribution in SNU-840 human ovarian cancer cells. The cell cycle was evaluated by flow cytometric DNA content analysis. SNU-840 cells were treated with daurinol (0-10 μM) or etoposide (200 μM) for 24 (A) and 48 h (B). Columns and error bars indicate the mean ± SD of three independent experiments. Statistics are based on ANOVA followed by Dunnett's test. *P<0.05, **P<0.01 and ***P<0.001 for the percentage of cells in each cell cycle phase compared with control.

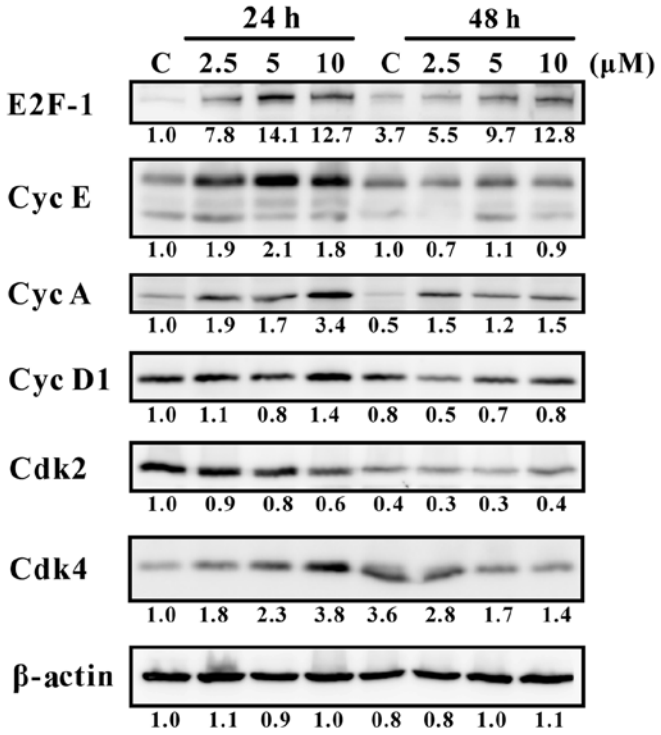

Figure 6. Effect of daurinol on the expression of cell cycle regulatory proteins. SNU-840 cells were treated with daurinol (2.5, 5 or 10 μM) for 24 and 48 h. Representative immunoblots are shown from at least three independent experiments. The relative protein expression was determined by densitometric analysis. C, vehicle control.

Daurinol induces increased expression of cyclin E, cyclin A and E2F-1 in SNU-840 cells. We also investigated the expression of cell cycle regulatory proteins such as cyclins and cyclin-dependent kinases to elucidate the molecular mechanism underlying the S phase arrest induced by daurinol in SNU-840 cells. Daurinol increased the expression of cyclins E and A (Fig. 6), which associate with Cdk2. The resulting complexes cyclin E/Cdk2 and cyclin A/Cdk2 regulate the initiation and progression of S phase, respectively (19,20). The expression of cyclin E was increased after 24 h of treatment; thus, we speculated that daurinol accelerated the initiation of S phase at 24 h. The expression of cyclin A was increased at both 24 and 48 h, suggesting that daurinol persisted in the enhanced S phase progression. In addition, daurinol increased E2F-1 expression at 24 and 48 h (Fig. 6). E2F-1 is a transcription factor that promotes the transcription of cyclin E and A (21). In summary, the enhanced expression of cyclin E, cyclin A and E2F-1 appear to be primarily responsible for the S phase arrest induced by daurinol.

Daurinol does not induce cell or nuclear enlargement in SNU-840 cells compared to etoposide. Finally, we investigated the effect of daurinol and etoposide on the cell and nuclear size of SNU-840 cells using microscopy and flow cytometry (15). Abnormal cell and nuclear enlargement was previously correlated with the side effects of anticancer agents (5). Microscopic observation showed that etoposide induced cell and nuclear enlargement in SNU-840 cells, while daurinol did not (Fig. 7A). To more accurately evaluate this phenomenon, we performed flow cytometric analysis of the fluorescence pulse signal in cells stained with DNA-binding fluorescent dye. The FSC-H values, which indicate the cell size, of etoposide-treated cells were higher than those of control or daurinol-treated cells (Fig. 7B); the mean values of FSC-H were 554.8±10.5, 587.3±19.6, 578.2±28.0, 604.6±44.2 and 743.3±33.9 for the control, 2.5, 5 and 10 μM daurinol and 10 μM etoposide-treated cells, respectively. Similarly, the FL2-W values (pulse width of PI fluorescence), which indicate the nuclear size (16), of etoposide-treated cells were higher than those of the control- or daurinol-treated cells (Fig. 7C); the mean FL2-H values were 197.4±4.5, 218.9±7.9, 237.0±14.4, 224.9±10.3 and 313.0±21.9 for the control, 2.5, 5 and 10 μM daurinol- and 10 μM etoposide-treated cells, respectively. Kolmogorov-Smirnov statistical analysis demonstrated that the FSC-H and FL2-W distributions of etoposide-treated cells were significantly different from those of the control or daurinol-treated cells. There was no significant difference between the control and daurinol-treated cells (Fig. 7D and E). Based on these data, we concluded that daurinol did not induce abnormal the cell or nuclear enlargement of SNU-840 cells, in contrast to etoposide.

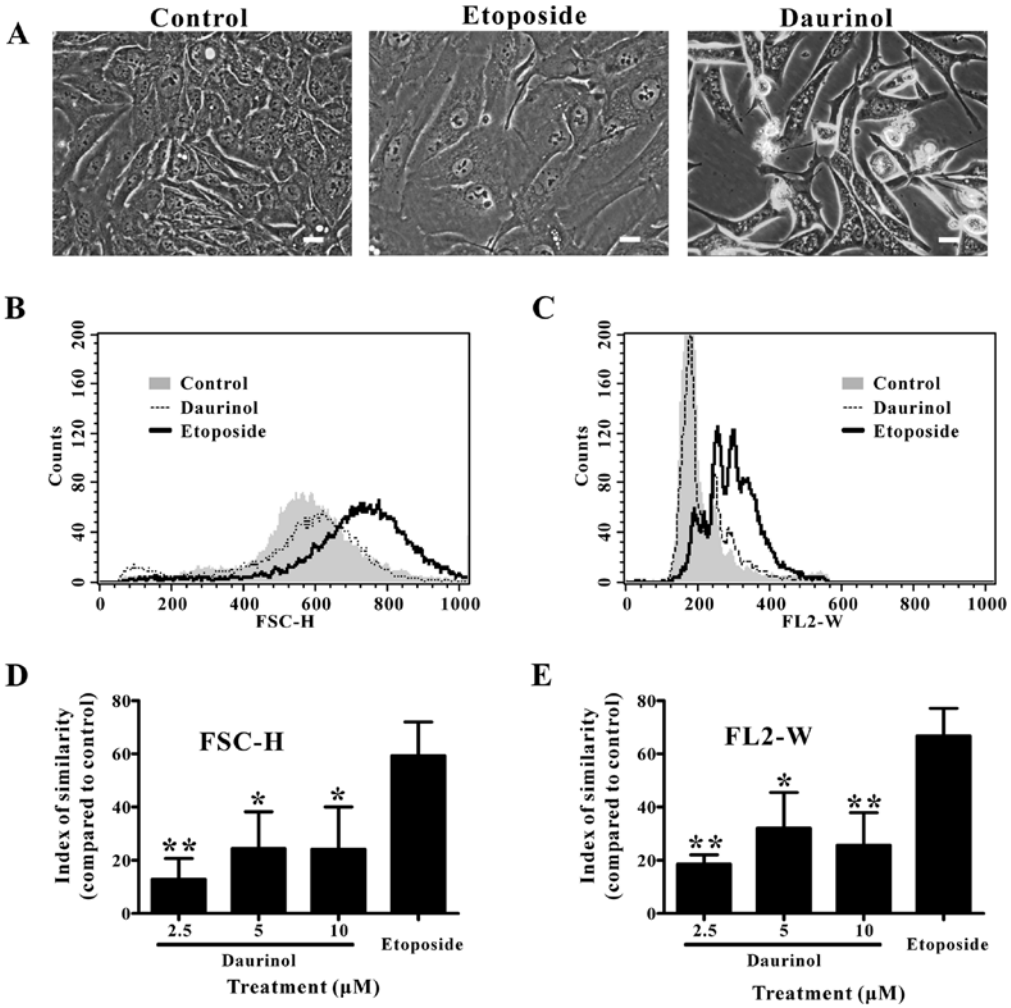

Figure 7. Effect of daurinol and etoposide on SNU-840 cell and nuclear size. (A) Phase contrast microscopy image of SNU-840 cells treated with daurinol (10 μM) or etoposide (10 μM) for 48 h (bar, 20 μm). (B-E) Flow cytometric analysis of the PI fluorescence pulse signal was used to evaluate the changes in the cell and nuclear size of SNU-840 cells induced by the treatment with daurinol (2.5, 5 and 10 μM) or etoposide (10 μM) for 48 h. (A, B) Histogram of FSC-H (A, cell size) and FL2-W (B, nuclear size) with gating on the singlet cell region. Overlay histograms schematized using control and daurinol (10 μM)- and etoposide (10 μM)-treated cell data. (C, D) Differences in the distributions of the FSC-H (C) and FL2-W (D) values between control and treated cells were quantitatively evaluated using Kolmogorov-Smirnov statistics. The index of similarity is the D/s(n) value of the Kolmogorov-Smirnov statistics. Columns and error bars indicate the mean ± SD of three independent experiments. Statistics were based on ANOVA followed by Tukey's test; *P<0.05 and **P<0.01 for significant differences from etoposide treatment.

Discussion

In the present study, we suggest the biochemical mechanism underlying the inhibitory action of micromolar daurinol against human topoisomerase IIα based on molecular docking studies and *in vitro* biochemical experiments. First, computational simulations predicted that daurinol might bind to the ATP-binding pocket of the enzyme. Second, a biochemical topoisomerase IIα assay revealed that increasing the concentration of ATP resulted in decreased inhibitory activity of daurinol against topoisomerase IIα. Third, determination of the amount of inorganic phosphate in the enzyme reaction mixture using the malachite green assay demonstrated that daurinol inhibited the ATP hydrolysis activity of topoisomerase IIα. Fourth, daurinol did not inhibit the activity of human topoisomerase I, which does not contain an ATP-binding domain. These properties of daurinol are similar to those reported for D11, a novel glycosylated diphyllin derivative (22). Taken together, these data demonstrate that daurinol inhibits human topoisomerase IIα by targeting its ATP-binding domain.

The molecular docking study also predicted that the benzodioxol functional group of daurinol interacts with a magnesium ion and the Lys168 residue of the enzyme; the naphthofuranone ring of daurinol overlaps with the adenine-binding site (Fig. 1C). Based on these data, we are synthesizing daurinol derivatives to test the binding model and to optimize inhibitory activity of topoisomerase and anticancer effects ultimately.

When optimizing lead compounds, several key factors must be considered. These factors include anticancer potency in appropriate cancer types; side effects such as hematological toxicity and drug-induced secondary leukemia; pharmacokinetic parameters; and physicochemical properties (solubility and stability). Especially, a rapid method for evaluating side effects is required prior to preclinical and

clinical toxicological assessment. In a previous study, we suggested that abnormal nuclear enlargement was correlated with the side effects of the topoisomerase inhibitors daurinol and etoposide in a human colorectal cancer model (5). In the present study, we confirmed that daurinol did not induce nuclear enlargement in SNU-840 human ovarian cancer cell line, in contrast to etoposide, which dramatically induced nuclear enlargement of SNU-840 cells. Therefore, we speculate that daurinol may be a potential candidate maintenance drug to treat ovarian cancer with minimal side effects. However, this method of assessing toxicity is limited because it uses cancer cells rather than normal tissue cells. To overcome this limitation, we suggest performing cell and nuclear size analysis in normal cells originating from human tissue or in a model animal such as *Caenorhabditis elegans* (23,24). *C. elegans* is frequently used for toxicity assessments of pharmaceutical compounds (24) and is compatible with flow cytometric DNA content analysis (25).

Etoposide-related secondary leukemia was recently reviewed. Although etoposide has been used successfully and extensively for the treatment of various cancers, secondary leukemia is a critical problem in clinical cancer treatment using topoisomerase inhibitors (3). The rearrangement of the mixed lineage leukemia (MLL) gene on chromosome 11q23 is associated with secondary leukemia. Similar to the author of that review, we also have hypothesized that prolonged maintenance of the abnormal enlarged nuclear status induced by etoposide may cause MLL gene rearrangement and the development of secondary leukemia. Because the previous (5) and present study confirmed that daurinol did not induce abnormal nuclear enlargement in either HCT116 or SNU-8 cells, daurinol may serve as a novel alternative to etoposide for the treatment of various cancers.

To evaluate daurinol as a novel alternative to the clinical anticancer drug etoposide, we investigated the anti-proliferative activity of ovarian, small-cell lung, and testicular cancer cells in addition to colorectal cancer, as etoposide is usually used to treat cancers other than colorectal cancer (5). Among the tested cancer cell lines, daurinol exerted more significant anti-proliferative activity than etoposide in human ovarian SNU-840 cells. Daurinol induced cell cycle arrest in S phase in SNU-840 cells, while etoposide induced G2/M phase arrest. These results are similar to previous reports in HCT116 human colorectal cancer cells (5).

In summary, we demonstrated that daurinol inhibited human topoisomerase IIα by interfering with ATP binding during the catalytic cycle of the enzyme. We also verified the potent anti-proliferative activity of daurinol in SNU-840 human ovarian cancer cells. Daurinol induced cell cycle arrest in S phase through the enhanced expression of cyclin E, cyclin A and E2F-1 in SNU-840 cells. However, daurinol did not induce abnormal nuclear enlargement compared to etoposide. Based on these data, we suggest that daurinol could be a novel alternative to the clinical anticancer agent etoposide. We hope that the results of this study can be exploited to develop daurinol and its derivatives as anticancer drugs to avoid the side effects of other topoisomerase II inhibitors, including hematological toxicity and secondary leukemia.

Acknowledgements

We gratefully acknowledge Dr Dulamjav Batsuren and Dr Jigjidsuren Tunsag of the Institute of Chemistry and Chemical Technology, Mongolia, for kindly providing natural daurinol. The present study was supported by an intramural grant from KIST (2Z04220), a grant from the Center Project for Korea-Mongolia Science and Technology Cooperation (Ministry of ICT, Science and Future Planning, Korea; 2U04650) and a grant from Gangneung Asan Hospital (Biomedical Research Center Promotion Fund).

References

1. Bailly C: Contemporary challenges in the design of topoisomerase II inhibitors for cancer chemotherapy. Chem Rev 112: 3611-3640, 2012.
2. Pogorelcnik B, Perdih A and Solmajer T: Recent advances in the development of catalytic inhibitors of human DNA topoisomerase IIα as novel anticancer agents. Curr Med Chem 20: 694-709, 2013.
3. Ezoe S: Secondary leukemia associated with the anti-cancer agent, etoposide, a topoisomerase II inhibitor. Int J Environ Res Public Health 9: 2444-2453, 2012.
4. Chen W, Qiu J and Shen YM: Topoisomerase IIα, rather than IIβ, is a promising target in development of anti-cancer drugs. Drug Discov Ther 6: 230-237, 2012.
5. Kang K, Oh SH, Yun JH, *et al*: A novel topoisomerase inhibitor, daurinol, suppresses growth of HCT116 cells with low hematological toxicity compared to etoposide. Neoplasia 13: 1043-1057, 2011.
6. Batsuren D, Batirov EK, Malikov VM, Zemlyanskii VN and Yagudaev MR: Arylnaphthalene lignans of *Haplophyllum dauricum*. The structure of daurinol. Chem Nat Compd 17: 223-225, 1981.
7. Graham JG, Quinn ML, Fabricant DS and Farnsworth NR: Plants used against cancer - an extension of the work of Jonathan Hartwell. J Ethnopharmacol 73: 347-377, 2000.
8. Hande KR: Etoposide: four decades of development of a topoisomerase II inhibitor. Eur J Cancer 34: 1514-1521, 1998.
9. Park JE, Lee J, Seo SY and Shin D: Regioselective route for arylnaphthalene lactones: convenient synthesis of taiwanin C, justicidin E, and daurinol. Tetrahedron Lett 55: 818-820, 2014.
10. Lanzetta PA, Alvarez LJ, Reinach PS and Candia OA: An improved assay for nanomole amounts of inorganic phosphate. Anal Biochem 100: 95-97, 1979.
11. Kang K, Jin YM, Jeon H, *et al*: The three proline residues (P25, P242, and P434) of Agrobacterium CP4 5-enolpyruvylshikimate-3-phosphate synthase are crucial for the enzyme activity. Plant Biotechnol Rep 4: 329-334, 2010.
12. Jun KY, Lee EY, Jung MJ, *et al*: Synthesis, biological evaluation, and molecular docking study of 3-(3'-heteroatom substituted-2'-hydroxy-1'-propyloxy) xanthone analogues as novel topoisomerase IIα catalytic inhibitor. Eur J Med Chem 46: 1964-1971, 2011.
13. Robinson MJ, Corbett AH and Osheroff N: Effects of topoisomerase II-targeted drugs on enzyme-mediated DNA cleavage and ATP hydrolysis: evidence for distinct drug interaction domains on topoisomerase II. Biochemistry 32: 3638-3643, 1993.
14. Kang K, Lee HJ, Kim CY, *et al*: The chemopreventive effects of *Saussurea salicifolia* through induction of apoptosis and phase II detoxification enzyme. Biol Pharm Bull 30: 2352-2359, 2007.
15. Kang K, Lee HJ, Yoo JH, *et al*: Cell and nuclear enlargement of SW480 cells induced by a plant lignan, arctigenin: evaluation of cellular DNA content using fluorescence microscopy and flow cytometry. DNA Cell Biol 30: 623-629, 2011.
16. Kang K, Lee SB, Yoo JH and Nho CW: Flow cytometric fluorescence pulse width analysis of etoposide-induced nuclear enlargement in HCT116 cells. Biotechnol Lett 32: 1045-1052, 2010.
17. Roca J: The mechanisms of DNA topoisomerases. Trends Biochem Sci 20: 156-160, 1995.

18. Larsen AK, Escargueil AE and Skladanowski A: Catalytic topoisomerase II inhibitors in cancer therapy. Pharmacol Ther 99: 167-181, 2003.
19. Eastman A: Cell cycle checkpoints and their impact on anti-cancer therapeutic strategies. J Cell Biochem 91: 223-231, 2004.
20. Masai H, Matsumoto S, You Z, Yoshizawa-Sugata N and Oda M: Eukaryotic chromosome DNA replication: where, when, and how? Annu Rev Biochem 79: 89-130, 2010.
21. DeGregori J, Kowalik T and Nevins JR: Cellular targets for activation by the E2F1 transcription factor include DNA synthesis- and G1/S-regulatory genes. Mol Cell Biol 15: 4215-4224, 1995.
22. Gui M, Shi DK, Huang M, *et al*: D11, a novel glycosylated diphyllin derivative, exhibits potent anticancer activity by targeting topoisomerase IIα. Invest New Drugs 29: 800-810, 2011.
23. Schmeisser S, Schmeisser K, Weimer S, *et al*: Mitochondrial hormesis links low-dose arsenite exposure to lifespan extension. Aging cell 12: 508-517, 2013.
24. Dengg M and van Meel JC: *Caenorhabditis elegans* as model system for rapid toxicity assessment of pharmaceutical compounds. J Pharmacol Toxicol Methods 50: 209-214, 2004.
25. van den Heuvel S and Kipreos ET: *C. elegans* cell cycle analysis. Methods Cell Biol 107: 265-294, 2012.